J. Membrane Biol. 164, 139–153 (1998)

The Journal of
Membrane
Biology

Modulation of I_A Potassium Current in Adrenal Cortical Cells by a Series of Ten Lanthanide Elements

J.J. Enyeart[1,2], L. Xu[1], J.C. Gomora[1], J.A. Enyeart[1]

[1]Department of Pharmacology, The Ohio State University College of Medicine, 5188 Graves Hall, 333 W. 10th Ave., Columbus, OH 43210-1239, USA

[2]The Neuroscience Program, The Ohio State University College of Medicine, Columbus, OH 43210-1239, USA

Received: 21 January 1997/Revised: 3 April 1998

Abstract. The modulation of I_A K^+ current by ten trivalent lanthanide (Ln^{3+}) cations spanning the series with ionic radii ranging from 0.99 Å to 1.14 Å was characterized by the whole-cell patch clamp technique in bovine adrenal zona fasciculata (AZF) cells. Each of the ten Ln^{3+}s reduced I_A amplitude measured at +20 mV in a concentration-dependent manner. Smaller Ln^{3+}s were the most potent and half-maximally effective concentrations (EC_{50}s) varied inversely with ionic radius for the larger elements. Estimation of EC_{50}s yielded the following potency sequence: Lu^{3+} (EC_{50} = 3.0 μM) ≈ Yb^{3+} (EC_{50} = 2.7 μM) > Er^{3+} (EC_{50} = 3.7 μM) ⩾ Dy^{3+} (EC_{50} = 4.7 μM) > Gd^{3+} (EC_{50} = 6.7 μM) ≈ Sm^{3+} (EC_{50} = 6.9 μM) > Nd^{3+} (EC_{50} = 11.2 μM) > Pr^{3+} (EC_{50} = 22.3 μM) > Ce^{3+} (EC_{50} = 28.0 μM) > La^{3+} (EC_{50} = 33.7 μM).

Ln^{3+}s altered selected voltage-dependent gating and kinetic parameters of I_A with a potency and order of effectiveness that paralleled the reduction of I_A amplitude. Ln^{3+}s markedly slowed activation kinetics and shifted the voltage-dependence of I_A gating such that activation and steady-state inactivation occurred at more depolarized potentials. In contrast, Ln^{3+}s did not measurably alter inactivation or deactivation kinetics and only slightly slowed kinetics of inactivated channels returning to the closed state. Replacement of external Ca^{2+} with Mg^{2+} had no effect on the concentration-dependent inhibition of I_A by Ln^{3+}s. In contrast to their action on I_A K^+ current, Ln^{3+}s inhibited T-type Ca^{2+} currents in AZF cells without slowing activation kinetics.

These results indicate that Ln^{3+} modulate I_A K^+ channels through binding to a site on I_A channels located within the electric field but which is not specific for Ca^{2+}. They are consistent with a model where Ln^{3+} binding to negative charges on the gating apparatus alters the voltage-dependence and kinetics of channel opening. Ln^{3+}s modulate transient K^+ and Ca^{2+} currents by two fundamentally different mechanisms.

Key words: Ion channels — Adrenal — Lanthanide — Potassium channel

Introduction

Trivalent cations including La^{3+} and the lanthanides (elements 58–71 in the periodic table) share biologically important chemical properties with the divalent calcium (Ca^{2+}) cation (Nieboer, 1975; Williams, 1982; Evans, 1990). Their similarity to Ca^{2+} with respect to ionic radii, coordination chemistry and preference for the oxygen donor groups provides the basis for their strong interaction with Ca^{2+} binding sites on membrane proteins (Nieboer, 1975; dos Remedios, 1981; Evans, 1990).

Ln^{3+} elements have been especially useful in the study of voltage-gated Ca^{2+} channels where they potently inhibit both low and high voltage-activated Ca^{2+} currents. In one extensive study, Ln^{3+}s were shown to inhibit low voltage-activated T-type Ca^{2+} channels through occlusion of the pore, with a potency that varies inversely with the ionic radius (Mlinar & Enyeart, 1993*b*). In contrast, the potency of L-type Ca^{2+} channel block by Ln^{3+} varies directly with ionic radii (Lansman, 1990).

Several reports suggest that Ca^{2+} may bind to specific sites on voltage-gated K^+ channels where they may be directly involved in voltage-dependent gating (Armstrong & Lopez-Barneo, 1987; Begenisich, 1988). Al-

Correspondence to: J.J. Enyeart

though systematic studies describing the effects of Ln^{3+} on voltage-gated K^+ currents have not been reported, La^{3+} has been shown to produce a depolarizing shift in the voltage dependence of activation and steady-state inactivation of a transient outward K^+ current in rat cerebellar neurons. La^{3+} was also reported to slow the activation and inactivation kinetics of this K^+ current (Watkins & Mathie, 1994).

Although some varieties of K^+ channels may contain Ca^{2+}-specific sites that are critically involved in gating, others may not (Mayer & Sugiyama, 1988). In addition to interacting with Ca^{2+}-binding sites, Ln^{3+}s bind with high affinity to other sites on selected proteins. Acetylcholine and insulin receptors possess two types of Ln^{3+} binding sites, only one of which accepts Ca^{2+} (Rubsamen et al., 1976; Williams & Turtle, 1984). Thus, Ln^{3+} modulation of voltage-gated K^+ channels might occur through receptors and mechanisms that differ fundamentally from their inhibition of Ca^{2+} channels.

We have examined the modulation of a rapidly inactivating A-type K^+ current by a series of 10 Ln^{3+}s which span the series and vary in ionic radii from 0.99 to 1.14 Å. Although Ln^{3+}s suppress I_A K^+ current with a potency that varies inversely with the ionic radius, the mechanism(s) involved are distinct from those that produce T-type Ca^{2+} channel inhibition.

Materials and Methods

Tissue culture media, antibiotics, fibronectin, and fetal bovine serum were obtained from Gibco BRL (Grand Island, NY). Culture dishes were purchased from Corning (Corning, NY). Coverslips were from Bellco (Vineland, NY). Lanthanide chlorides (at least 99.9% purity) were obtained from Aldrich Chemical (Milwaukee, WI). All other chemicals were purchased from Sigma (St. Louis, MO). The rat medullary thyroid carcinoma 6–23 (clone 6) cell line (rat C cells) was purchased from the American Type Culture Collection.

Isolation and Culture of Cells

Bovine adrenal glands were obtained from steers (age range 1 to 3 years) within 15 min of slaughter at a local slaughterhouse. Fatty tissue was removed immediately and the glands were transported to the laboratory in ice-cold PBS containing 0.2% dextrose. Isolated AZF cells were prepared as previously described with some modifications (Gospodarowicz et al., 1977). In a sterile tissue culture hood, the adrenals were cut in half lengthwise and the lighter medulla tissue trimmed away from the cortex and discarded. The capsule with attached glomerulosa and thicker fasciculata-reticularis layer were then dissected into large pieces approximately 1.0 × 1.0 × 0.5 cm. A Stadie-Riggs tissue slicer (Thomas Scientific) was used to slice fasciculata-reticularis tissue from the glomerulosa layers by slicing 0.3 to 0.5 mm slices from the larger pieces. The first medulla/fasciculata slices were discarded. One to two subsequent fasciculata slices were saved in cold sterile PBS/0.2% dextrose. Fasciculata tissue slices were then diced into 0.5 mm^3 pieces and dissociated with 2 mg/ml (about 200–300 U/ml) of Type I collagenase (neutral protease activity not exceeding 100 units/mg of solid), 0.2 mg/ml deoxyribonuclease in DMEM/F12 for approximately 1 hr at 37°C, triturating after 30 and 45 min with a sterile, plastic transfer pipette. After incubating, the suspension was filtered through 2 layers of sterile cheesecloth, then centrifuged to pellet cells at 100 × *g* for 5 min. Undigested tissue remaining in the cheesecloth was incubated with collagenase (2 mg/ml) for an additional hour. Pelleted cells were washed twice with DMEM/0.2% BSA, centrifuging as before. Cells were filtered through 200 μm stainless steel mesh to remove clumps after resuspending in DMEM. Dispersed cells were again centrifuged and either resuspended in DMEM/F12 (1:1) with 10% FBS, 100 U/ml penicillin, 0.1 mg/ml streptomycin and plated for immediate use of resuspended in FBS/5% DMSO, divided into 1-ml aliquots each containing about 2×10^6 cells and stored in liquid nitrogen for future use. Cells were plated in 35-mm dishes containing 9 mm^2 glass coverslips that had been treated with fibronectin (10 μg/ml) at 37°C for 30 min then rinsed with warm, sterile PBS immediately before adding cells. Dishes were maintained at 37°C in a humidified atmosphere of 95% air and 5% CO_2. Rat thyroid 6–23 C cells were cultured as previously described (Biagi & Enyeart, 1991).

Solutions and Bath Perfusion

For recording whole-cell K^+ currents, the standard pipette solution was (in mM): 120 KCl, 2 $MgCl_2$, 1 $CaCl_2$, 10 HEPES, 11 BAPTA, 200 μM GTP, 2 mM MgATP with pH buffered to 7.2 using KOH. With this composition, free $[Ca^{2+}]$ was determined to be 2.3×10^{-8} M using the ''Bound and Determined'' program (Brooks & Storey, 1992). The development of the noninactivating I_{AC} K^+ current that is present in these cells was completely eliminated by including 200 μM cAMP in the pipette solution. cAMP selectively inhibits the I_{AC} K^+ current and does not alter I_A (Enyeart, Mlinar & Enyeart, 1996). Pipette solutions were filtered through 0.22 micron cellulose acetate filters. The external solution consisted of (in mM): 140 NaCl, 5 KCl, 2 CaCl, 2 $MgCl_2$, 10 HEPES and 5 glucose, pH 7.4 using NaOH.

T-type Ca^{2+} currents were recorded from AZF cells or the rat thyroid 6–23 cell line were recorded as previously described (Biagi & Enyeart, 1991; Mlinar, Biagi & Enyeart, 1993).

Handling of lanthanides is restricted by their chemical properties (Evans, 1990). To avoid formation and precipitation of insoluble $Ln(OH)_3$ and $Ln(CO)_3$, as well as formation of radiocolloids and loss of Ln^{3+} ions to the container surface, millimolar aqueous stock solutions of $LnCl_3$ were prepared daily in polyethylene microtubes. Stock solutions were diluted to final concentration directly in the bath perfusion vessel immediately before use. The perfusion system consisted of polyethylene and polypropylene containers and tubing, since Y^{3+}, La^{3+} and the lanthanides strongly bind to negatively charged groups or glass surfaces. The recording chamber (volume ≈ 1 ml) was continuously perfused by gravity at a rate of 5–6 ml/min. Bath solution exchange was done by a manually controlled six-way rotary valve.

Despite the relatively constant activity coefficients of trivalent lanthanide chlorides in aqueous solution and precautions taken in experimental procedures, free concentration of unhydrolyzed $Ln(H_2O)_n^{3+}$ ionic species in the extracellular solution cannot be determined with certainty. Partial hydrolysis of Ln^{3+}s results in rapid formation of relatively soluble $Ln(OH)^{2+}$, $Ln(OH)_2^+$ and other species (Evans, 1990; Biedermann & Ciavatta, 1961), the final concentrations of which are unknown. It is possible that some of the hydrolysis products contributed to the observed effects in this study.

Recording Conditions and Electronics

AZF cells were used for patch clamp experiments 2–12 hr after plating. Coverslips with cells were transferred from 35-mm culture dishes to the

recording chamber. Cells with diameters of 15–20 μm in diameter and capacitances of 8–15 pF were used for recording. Patch electrodes with resistances of 1–2 megohms were fabricated from 0010 glass (Corning) using a Brown-Flaming Model P-80 microelectrode puller (Sutter Instruments, Novato, CA). Access resistance during recording estimated from the transient cancellation controls of the patch clamp amplifier was 2–5 megohms. The combination of access resistance and cell capacitance yielded voltage clamp time constants of <100 μs.

Whole cell currents were recorded at room temperature (22–24°C) following the procedure of Hamill et al. (1981), using a List EPC-7 (List-Medical, Darmstadt, Germany) patch clamp amplifier. Pulse generation and data acquisition were done with a personal computer and PCLAMP software with an Axolab interface (Axon Instruments). Currents were digitized at 1–50 kHz after filtering with an 8-pole Bessel filter (Frequency Devices, Haverhill, MA). Linear leak and capacity currents were subtracted from current records using summed scaled hyperpolarizing steps of ½ to ¼ pulse amplitude.

Data were analyzed using PCLAMP 5.5 and 6.03 (CLAMPAN and CLAMPFIT) and GraphPAD Inplot 4 (GraphPAD Software, San Diego, CA). All fits to single exponential functions were done using the PCLAMP least-squares regression subroutine. Inhibition curves are InPlot 4 least-square regression fits, where current in control saline is normalized to 1, and assuming complete block of current with sufficient concentration of antagonists. All quantitative results are given as the mean ± SEM or, in the case of least-square fits, as the estimate ± SEE (standard error of the estimate).

Abbreviations

EC_{50}	half-maximally effective concentration
Ln^{3+}	lanthanide
I_A	inactivating potassium current in bovine adrenal fasciculata cells
AZF	bovine adrenal fasciculata
ATP-γ-S	Adenosine 5′O-(-3-thiotriphosphate)
DMEM	Dulbecco's modified eagle medium
DMEM/F12+	DMEM/F12 (1:1) containing 10% FBS, 100 U/ml penicillin, 0.1 mg/ml streptomycin and the antioxidants 1 μM tocopherol, 20 nM selenite and 100 μM ascorbic acid
BAPTA	1,2-bis-(2-aminophenoxy)ethane-N,N,N′,N″-tetraacetic acid
IV	current-voltage relationship
IIV	instantaneous current/voltage relationship
FBS	fetal bovine sera

Results

Ln^{3+}s Suppress I_A Current

In whole-cell patch clamp experiments, each of the ten Ln^{3+} elements rapidly reduced I_A amplitude in a concentration-dependent manner (Fig. 1). Inhibition by less potent Ln^{3+}s such as La^{3+} was rapidly and nearly completely reversible upon switching to control saline (Fig. 1*A*). Inhibition by more potent Ln^{3+}s such as Yb^{3+} was only partially reversed after prolonged washing (Fig. 1*C*).

To quantitate the relative potency of the Ln^{3+} ions in reducing I_A current, inhibition curves were constructed for each of the ten elements after measuring I_A at Ln^{3+} concentrations ranging from 1 to 500 μM. EC_{50}s varied over a more than 10-fold range from 2.74 ± 0.20 μM ($n = 7$) for Yb^{3+} to 33.7 ± 4.8 μM ($n = 7$) for La^{3+} (Fig. 2*A*). The potency of the Ln^{3+}s in reducing I_A amplitude varied inversely with the ionic radii of these ten metal cations (Fig. 2*B*). This inverse relationship was most evident for Ln^{3+}s with ionic radii between 1.160 Å (La^{3+}) and 1.079 Å (Sm^{3+}) where EC_{50}s ranged from 33.7 μM ± 4.8 ($n = 7$) to 6.86 ± 1.36 μM ($n = 7$). For the remaining smaller elements with ionic radii ranging from 1.055 Å (Gd^{3+}) down to 0.977 Å (Lu^{3+}), EC_{50}s decreased much more gradually (Fig. 2*B*).

Ln^{3+}s and Activation Kinetics

The concentration-dependent reduction of I_A amplitude produced by each of the Ln^{3+}s, measured at a single test potential (+20 mV) could have occurred through any of several different mechanisms. Besides occluding the channel pore, Ln^{3+}s might suppress I_A K^+ current through modulation of the steady-state voltage dependence or kinetics of channel gating.

In viewing whole-cell recordings, it was obvious that, in addition to reducing I_A amplitude, each of the ten Ln^{3+}s also slowed the activation kinetics of this current (Fig. 3*A*). Activation kinetics of I_A in AZF cells is described by an equation of the form (Mlinar & Enyeart, 1993*b*):

$$I = I_{MAX}[1 - \exp(-T/\tau_a)]^4$$

Quantitation of activation kinetics is complicated by the overlapping process of open channels progressing rapidly to the inactivated state. However, I_A inactivation kinetics are independent of voltage over a wide range of membrane potentials (Mlinar & Enyeart, 1993*b*). A large fraction (≈80%) of I_A inactivation occurs with a rapid time constant (10–15 msec) (Mlinar & Enyeart, 1993*b*) which is not altered by trivalent Ln^{3+}s (*see* Figs. 6 and 7 and corresponding Results below). Therefore, the early phase of I_A current (0–20 msec) recorded in response to depolarizing steps to +20 mv could be nicely fit by the formula: $I = I_{MAX}[1 - \exp(-T/\tau_a)]^4[\exp(-T/\tau_i)]$, where τ_i is the voltage-dependent and Ln^{3+}-insensitive inactivation time constant obtained from fits of the inactivating component of I_A measured at +20 mV in control saline (Fig. 3*B*).

The effectiveness of the Ln^{3+}s in slowing activation kinetics varied inversely with ionic radii, and this relationship was again especially apparent for the larger elements. In Fig. 3, superfusing the cell with 10 μM La^{3+} (ionic radius 1.16 Å) increased τ_a from 0.91 msec to 2.19 msec. In comparison, 10 μM Sm^{3+} (ionic radius 1.079 Å) increased τ_a from 1.04 msec to 6.11 msec.

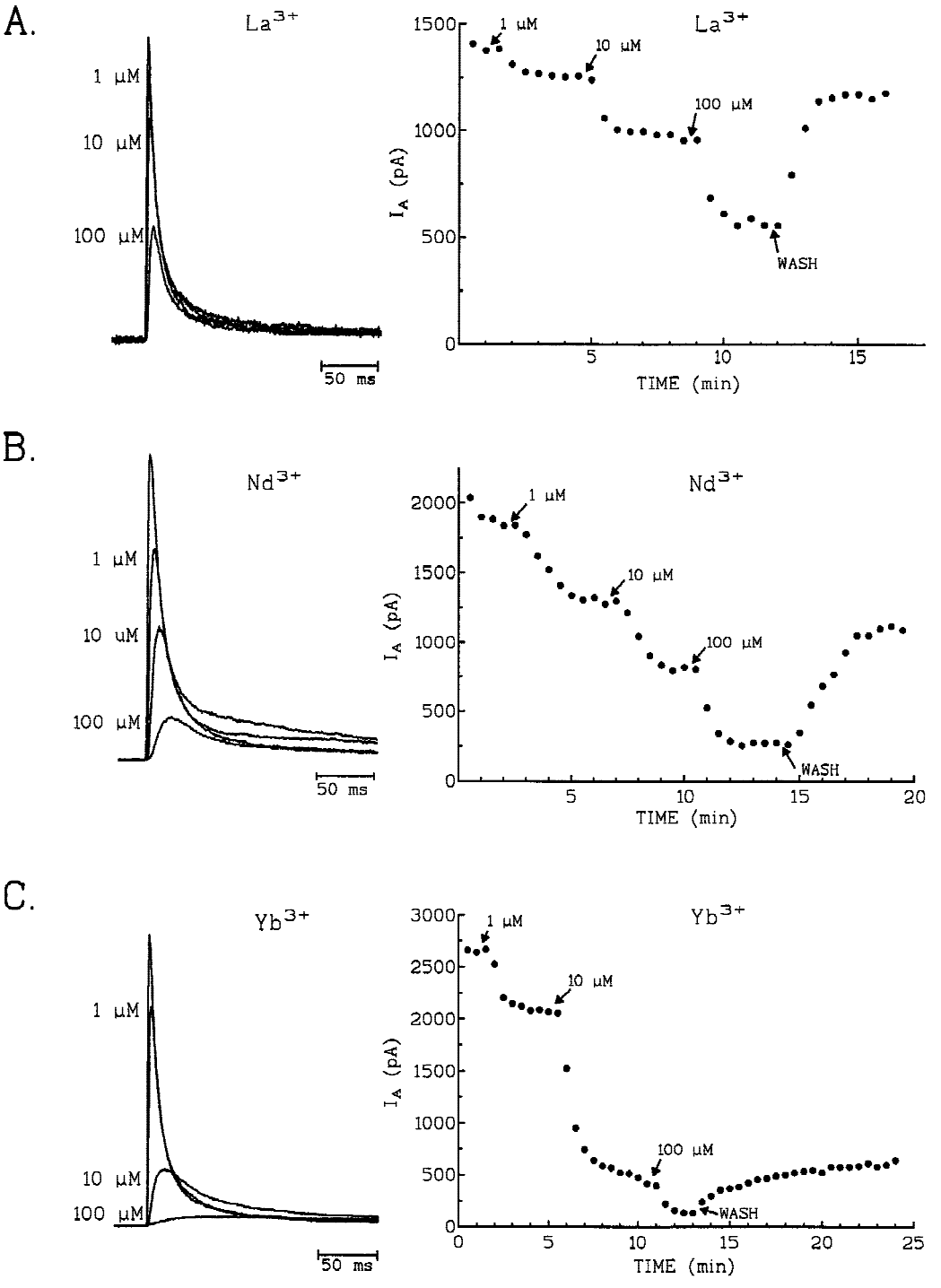

Fig. 1. Concentration-dependent inhibition of I_A K^+ current by Ln^{3+}s in bovine AZF cells. I_A was activated from a holding potential of −80 mV by voltage steps to +20 mV, applied at 30-sec intervals. Cells were superfused with: (*A*) La^{3+}; (*B*) Nd^{3+}; or (*C*) Yb^{3+} at concentrations of 1, 10 or 100 μM with continuous recording of I_A current. The averaged current traces represent the steady-state current at the indicated Ln^{3+} concentration. Peak current amplitudes are plotted against time at right and show effect of superfusing control saline at the indicated time (wash).

Slowing of activation kinetics by Ln^{3+}s was concentration-dependent and indicative of increased potency of the smaller Ln^{3+} elements. At concentrations of 1, 10 and 100 μM, Sm^{3+} increased τ_a from a control value of 1.14 ± 0.12 msec (n = 4) to values of 2.76 ± 0.21, 5.41 ± 0.50 and 9.20 ± 0.02 msec, respectively. By contrast, La^{3+} at the same three concentrations increased τ_a from its control value of 1.09 ± 0.09 msec (n = 3) to

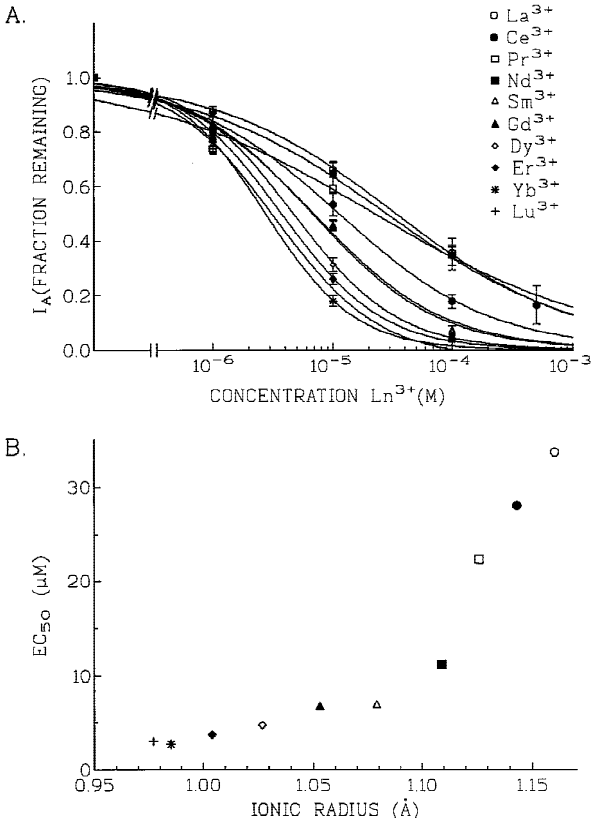

Fig. 2. Concentration-dependent inhibition of I_A by Ln^{3+}s and relationship to ionic radius. (*A*) Inhibition curves for 10 Ln^{3+} ions. Data obtained in experiments as described in the legend of Fig. 1. Data points are normalized mean values obtained in 4–7 separate measurements after steady-state block was reached. Inhibition curves are best fits of the data to an equation of the form: $Y = 1/1 + (X/EC_{50})^h$ where Y is the fraction of control current remaining after addition of the antagonist, and X is the Ln^{3+} concentration and h is the Hill slope. EC_{50}s have been estimated from the fits, and these are: La^{3+}, 33.7 ± 4.8 μM; Ce^{3+}, 28.0 + 4.1 μM; Pr^{3+}, 22.3 ± 10.4 μM; Nd^{3+}, 11.2 ± 1.9 μM; Sm^{3+}, 6.86 ± 1.36 μM; Gd^{3+}, 6.71 ± 1.59 μM; Dy^{3+}, 4.66 ± 0.37 μM; Er^{3+}, 3.72 ± 0.33 μM; Yb^{3+}, 2.74 ± 0.20 μM; Lu^{3+}, 2.97 ± 0.17 μM. Hill coefficients varied monotonically and ranged from 0.571 for La^{3+} to 1.267 for Lu^{3+}. (*B*) Potency as a function of ionic radius. EC_{50}s of the 10 Ln^{3+}s are plotted against corresponding cationic radius (Shannon, 1976), assuming a coordination number of 8. While 8 is the most likely coordination number for Ln^{3+}s (Nieboer, 1975), the presence of ionic species with other coordination numbers is probable. Symbols of EC_{50}s are the same as in (*A*) above.

1.15 ± 0.12, 2.42 ± 0.20 and 5.96 ± 0.45 msec, respectively.

Overall, the increase in τ_as produced by seven Ln^{3+} elements at a concentration of 10 μM (expressed as a ratio of the control value) ranged from 2.24 ± 0.18 ($n = 3$) for La^{3+} to 6.01 ± 1.05 for Yb^{3+} ($n = 3$) (Fig. 3*C*). The inverse relationship between size and slowing of activation kinetics was again most evident among the larger elements with ionic radii between 1.079 Å and 1.160 Å.

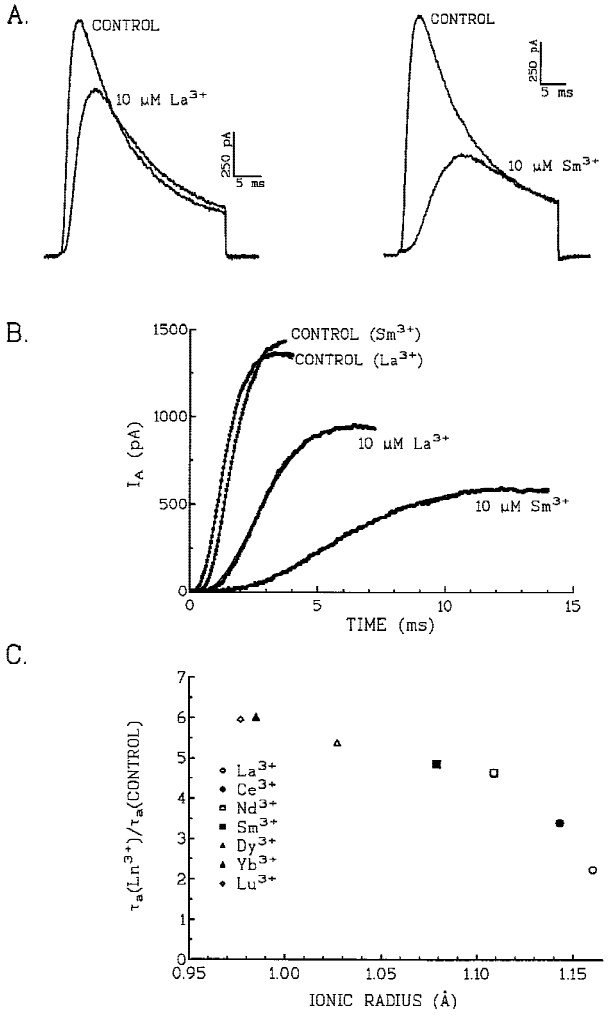

Fig. 3. Effect of Ln^{3+}s on I_A activation kinetics. The effect of La^{3+} (10 μM) and Sm^{3+} (10 μM) on the kinetics of I_A activation were studied in whole-cell recordings by applying activating voltage steps from a holding potential of −80 mV to a test potential of +20 mV before and after superfusing cells with Ln^{3+}s. The ascending portion of I_A current was fit from time = 0 with an equation of the form: $I = I_\infty[1 - \exp(-T/\tau_a)]^4[\exp(-T/\tau_i)]$ where I_∞ is the maximum value that the current would reach in the absence of inactivation, τ_a is the voltage-dependent time constant of activation and τ_i is a voltage-independent inactivation time constant obtained by fitting the inactivating component of I_A, measured at +20 mV in control saline. (*A*) Current records before and after superfusing cells with 10 μM La^{3+} (left traces) or 10 μM Sm^{3+} (right traces). (*B*) Same currents as in (*A*) displayed on an expanded time scale. Solid lines show best fits to above equation with respective τ_as of 2.19 and 6.11 for La^{3+}- and Sm^{3+}-treated cells. (*C*) Activation time constants obtained for I_A currents in the presence of 10 μM Ln^{3+} are expressed as a ratio of control value and plotted against ionic radius for 8 Ln^{3+}s. Values are mean ± SEM, for 3–5 determinations.

The activation kinetics of I_A are voltage-dependent and accelerated at progressively more positive test potentials (Mlinar & Enyeart, 1993*b*). Figure 4 illustrates the effect of 10 μM Dy^{3+} (ionic radius 1.027 Å) on I_A K^+ current amplitudes and activation kinetics at test poten-

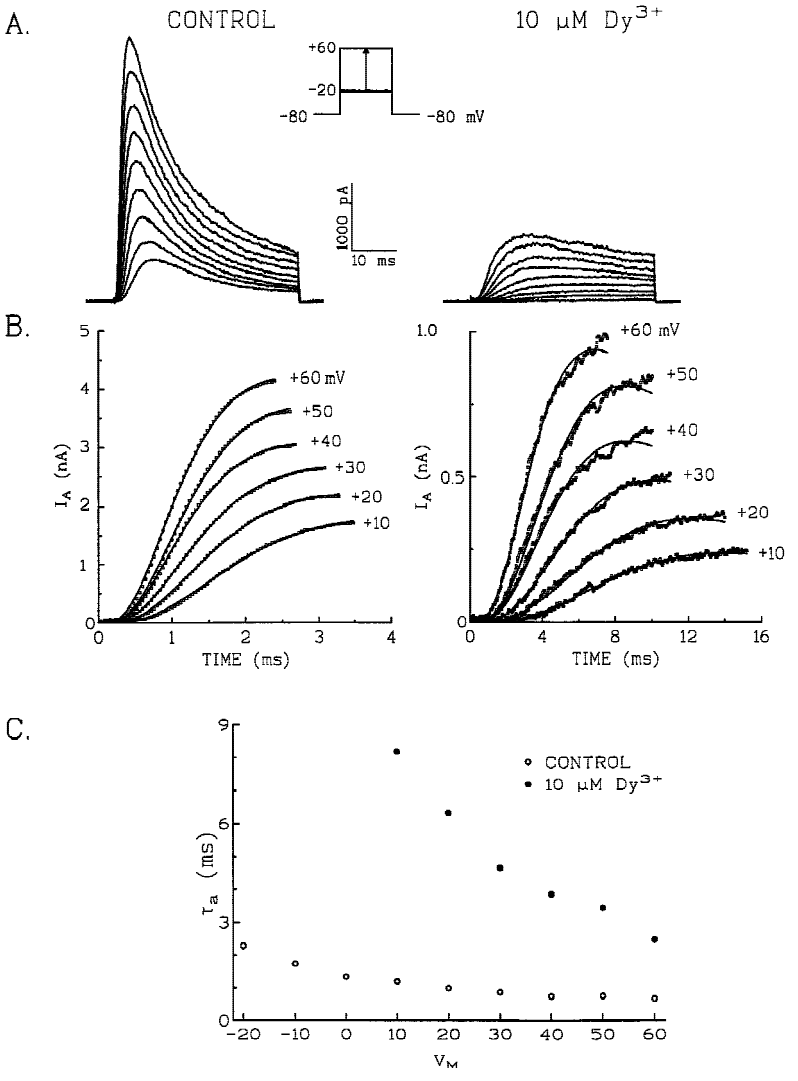

Fig. 4. Effect of Dy^{3+} on voltage-dependent activation kinetics. I_A currents were recorded in response to voltage steps to test potentials between −20 and +60 mV, applied from a holding potential of −80 mV before and after superfusing 10 μM Dy^{3+}. Activation time constants were determined by fitting the ascending component of I_A current with the equation described in the legend of Fig. 3. (*A*) Current records at test potentials between −20 and +60 mV before and after superfusing 10 μM Dy^{3+}. (*B*) Activating portion of I_A and corresponding fits (solid lines) at indicated test potentials for same cell as in (*A*). (*C*) Activation time constants (τ_as) derived from fits in (*B*) and plotted against test potential.

tials between −20 and +60 mV. Activation kinetics for I_A were fit as in Fig. 3 above. In control saline, τ_as obtained from fits varied from 2.28 msec at −20 mV to 0.66 msec at +60 mV (Fig. 4*B*,*C*). After superfusing 10 μM Dy^{3+}, τ_as ranged from 8.17 msec at +10 mV (the most negative potential for which reliable fits could be obtained) to 2.48 msec at +60 mV. Thus, 10 μM Dy^{3+} produced the equivalent of an approximate 80 mV shift in I_A activation kinetics (Fig. 4*C*). Similar results were obtained in each of 3 cells.

Ln^{3+}s and Inactivation Kinetics

In a previous study, we found that the major fraction of I_A (>80%) inactivates with a single voltage-independent fast time constant (Mlinar & Enyeart, 1993*b*). In the present study, we found that the Ln^{3+}s do not measurably alter the inactivation kinetics of I_A. Figure 5 illustrates the effect of Ce^{3+} (10 μM) on the decaying phase of I_A current measured at test voltages between −20 and +60 mV. In control saline, I_A inactivation was fit with a single exponential time constant that did not change significantly over the entire range of test voltages, with τ_is ranging from 10.5 ± 2.1 msec to 12.3 ± 2.4 msec (n = 3) (Fig. 5*A* and *B*). In the presence of Ce^{3+} (10 μM), I_A inactivation kinetics at negative potentials (−20 to 0 mV) appeared to be markedly slowed, while τ_is approached control values at more positive potentials (Fig. 5*B*). These results suggested that the apparent Ce^{3+}-induced slowing of inactivation at negative voltages occurred as a consequence of slowed activation at these potentials.

To determine if the apparent slowed inactivation of I_A produced by Ce^{3+} at negative test voltages was an outcome of slowed and prolonged activation, we measured inactivation kinetics in 10 μM Ce^{3+} at potentials between −20 and −10 mV after I_A activation had been

accelerated by a 5-msec prepulse to +40 mV. Under these conditions, τ_is approached the same voltage-independent time constant in the presence and absence of Ce^{3+}. In the experiment illustrated in Fig. 6, I_A inactivation was measured at −10 mV with (Fig. 7*B*) and without (Fig. 7*A*) a 5-msec prepulse to +40 mV before and after superfusing 10 μM Ce^{3+} as indicated. Without the accelerating prepulse, the inactivating component of I_A was fit with single time constants of 13.9 and 42 msec in control saline and in 10 μM Ce^{3+}, respectively (Fig. 6*A*). By comparison, when the voltage protocol included the accelerating prepulse, the inactivating phase of I_A (measured at −10 mV) was fit with time constants of 12.3 msec before, and 15.7 msec after exposure to $CeCl_3$ (Fig. 6*B*).

Overall, when inactivation was measured at potentials between −20 and −10 mV, after a 5 msec prepulse to +40 mV, τ_is in control saline and 10 μM Ce^{3+} were 13.6 ± 0.9 msec and 12.9 ± 1.5 msec ($n = 4$). Thus, when activation was accelerated by strong depolarization, Ce^{3+} had no effect on I_A inactivation kinetics even at relatively negative potentials.

Effect of Ln^{3+}s on Recovery and Deactivation Kinetics

In contrast to their marked slowing of activation kinetics, Ln^{3+} had little impact on the kinetics of inactivated K^+ channels returning to their closed state. Recovery kinetics were studied by first clamping cells at −20 mV for 30 sec to inactivate I_A, then stepping the membrane potential to −80 mV for various periods up to 30 sec, before applying an activating test pulse to +20 mV (Fig. 7*A*). Recovery kinetics in control saline and in the presence of 10 μM Ce^{3+} were fit with single exponential time constants of 9.3 ± 0.3 sec and 8.8 ± 0.3 sec respectively ($n = 3$) (Fig. 7*A* and *B*). While Ce^{3+} had no measurable effect on τ_r, the smaller Ln^{3+}s, Dy^{3+} (10 μM) slightly slowed τ_r from 10.1 ± 0.2 sec to 13.5 ± 0.4 sec ($n = 3$) (Fig. 7*C*).

Ln^{3+}s failed to alter the closing kinetics of I_A channels that had been opened by depolarization. In these experiments, deactivating ''tail'' currents were recorded at −50 mV after activating I_A channels with a short 5-msec voltage step to +50 mV in control saline and after superfusing 1 and 10 μM Gd^{3+}. In the absence of Ln^{3+}s, I_A channels relaxed to the closed state through a process fit by a single exponential with a time constant (τ_d) of 9.5 ± 0.9 msec ($n = 3$). By comparison, in these same cells, I_A deactivated with time constants of 10.94 ± 1.48 msec and 10.28 ± 1.15 msec after superfusing Gd^{3+} at 1 μM and 10 μM, respectively.

Effect of Ln^{3+}s on Voltage-dependent Steady-State Inactivation and Activation

Ln^{3+} shifted the voltage-dependence of steady-state inactivation to the right along the voltage axis. This shift

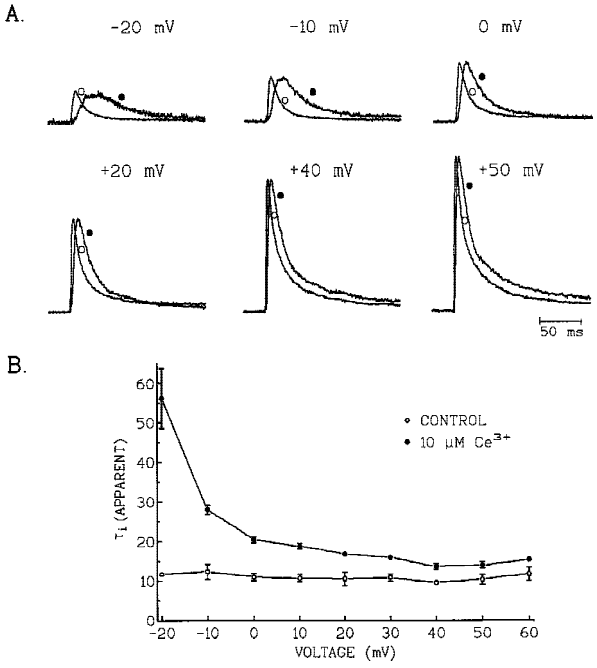

Fig. 5. Ce^{3+} and I_A inactivation kinetics. (*A*) I_A was activated from a holding potential of −80 mV by voltage steps to potentials between −20 and +60 mV applied at 30-sec intervals in control saline and after superfusing 10 μM Ce^{3+}. Traces show scaled currents in control saline and in the presence of Ce^{3+} as indicated. (*B*) The decaying phase of I_A was fit with a single exponential to determine the apparent inactivation time constant (τ_i). τ_is are plotted against membrane potential. Values are mean ± SEM, for $n = 3$.

was concentration-dependent and again greatest with the smaller Ln^{3+}s. Voltage-dependent inactivation of I_A was quantitated by applying 10-sec conditioning pulses to various potentials between −82.5 and −7.5 mV in 7.5 mV increments, followed by activating voltage steps to +20 mV. The normalized current was plotted as a function of the conditioning voltage and fitted with a Boltzmann equation. Figure 8*A* and *B* illustrate an experiment in which 10 and 100 μM Pr^{3+} shifted the midpoint of the steady-state inactivation curve by 19.6 mV and 39.1 mV, respectively. Overall, at 10 μM, two of the larger Ln^{3+}s, Ce^{3+} and Pr^{3+}, shifted the $v_{1/2}$s of steady-state inactivation by 14.8 ± 1.3 mV ($n = 3$) and 21.3 ± 2.0 mV ($n = 3$), respectively. By comparison, the smaller elements, Nd^{3+} and Er^{3+} shifted $v_{1/2}$ by 26.1 ± 0.8 mV ($n = 6$) and 30.3 ± 2.5 mV ($n = 6$), respectively (Fig. 8*C*).

Voltage-dependent Activation

Current-voltage relationships obtained in the absence and presence of Ln^{3+}s indicated that these elements produced a rightward shift along the voltage axis in the threshold for I_A activation. Further, Ln^{3+}s became less effective at reducing I_A amplitude at progressively more

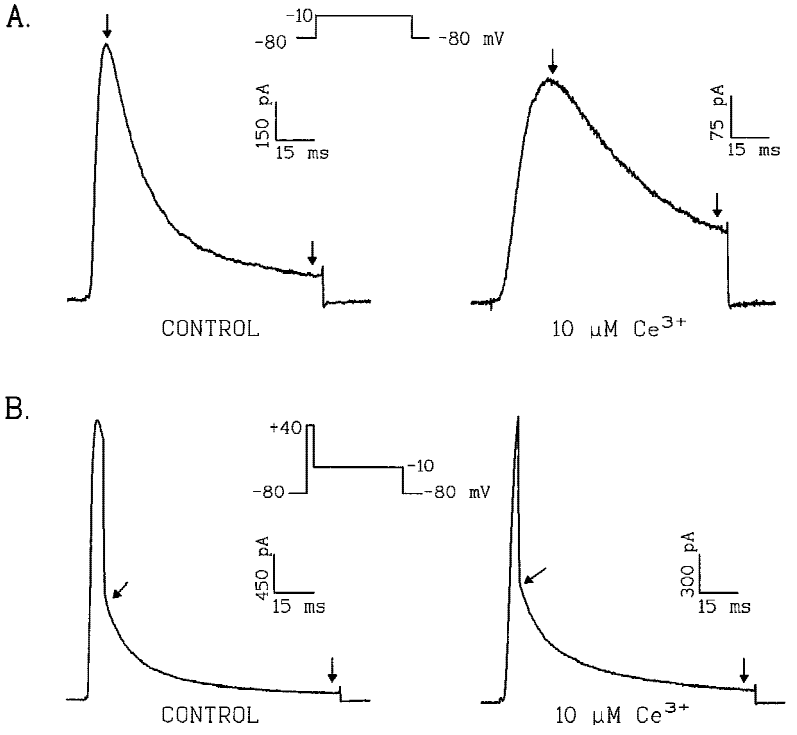

Fig. 6. Effect of activating voltage on τ_i. I_A currents were activated from −80 mV by a single voltage step of 40-msec duration to a test potential of −10 mV (*A*) or by an identical voltage step preceded by a 5 msec prepulse to +40 mV (*B*). Both protocols were applied to the cell before and after superfusing 10 μM Ce^{3+}. The inactivating component of I_A measured at −10 mV in each case was fit with a single exponential between the points demarcated by arrows on each of the traces.

positive test potentials (Fig. 9). Both of these effects are consistent with a Ln^{3+}-induced depolarizing shift in the voltage dependence of I_A open probability. Again, the smaller Ln^{3+}s were more effective at altering the apparent threshold for I_A activation and reducing I_A amplitude at all voltages. Specifically, Ce^{3+} (10 μM) and Lu^{3+} (10 μM) altered the threshold for I_A activation by approximately +20 and 40 mV respectively (Fig. 9*A* and *C*). Dy^{3+} and Gd^{3+} produced intermediate shifts. Similarly, Ce^{3+} reduced I_A amplitude by 48.7 ± 2.5% and 29.3 ± 6.4% ($n = 3$) at test potentials of 0 and +60 mV respectively. By comparison, Lu^{3+} reduced I_A by 89.6 ± 1.9% and 77.2 ± 5.8% ($n = 3$) at these same voltages. Dy^{3+} was again intermediate in potency, reducing I_A by 80.2 ± 9.0% and 64.4 ± 9.5% ($n = 3$) and 0 and +60 mV.

The diminished effectiveness of the Ln^{3+}s in reducing I_A amplitude at progressively more depolarized potentials suggested that these agents altered the voltage-dependence of I_A activation by shifting the channel activation or fraction open curve to the right along the voltage axis. It is difficult to accurately determine the steady-state voltage dependence of activation of a rapidly-inactivating current. In this regard, we discovered that substituting the nonhydrolyzable ATP analog ATP-γ-S for ATP in the pipette solution markedly slowed I_A inactivation kinetics over a period of minutes in about one-third of the cells tested (Fig. 10*A*, left traces). We studied the effect of Ce^{3+} (10 μM) and Dy^{3+} (10 μM) on the voltage dependence of activation in cells where I_A activation kinetics had been dramatically slowed by ATP-γ-S.

The voltage dependence of opening was determined by applying activating voltage steps of various size from a holding potential of −80 mV, and then stepping the voltage back to a constant potential (−50 mV) where the tail current was measured (Fig. 10*A*). The tail current amplitude is directly proportional to the number of channels that are open at the end of the activating pulse.

Fraction open curves were obtained by plotting the initial amplitude of the tail current as a function of the membrane potential during the activating voltage step. Tail current amplitudes were normalized and expressed as the fraction of open channels, plotted against membrane potential and fit by a Boltzmann function of the form:

$$\text{fraction open} = 1/[1 + \exp(v_{1/2} - v)/K]^4$$

where $v_{1/2}$ is the voltage where half of the single gate sensors are in the open configuration and K is the slope factor (Mlinar & Enyeart, 1993b). Curves were fit to data points acquired at test potentials between −50 and +60 mV. In Fig. 10*B*, Ce^{3+} (10 μM) shifted the midpoint of the fraction open curve by +24 mV, while Dy^{3+} produced a +48 mV shift.

Mechanism of Ln^{3+} Action

The inhibition of I_A K^+ current in AZF cells resembles the inhibition of T-type Ca^{2+} current in thyroid C cells by Ln^{3+}s where the potency also varies inversely with the

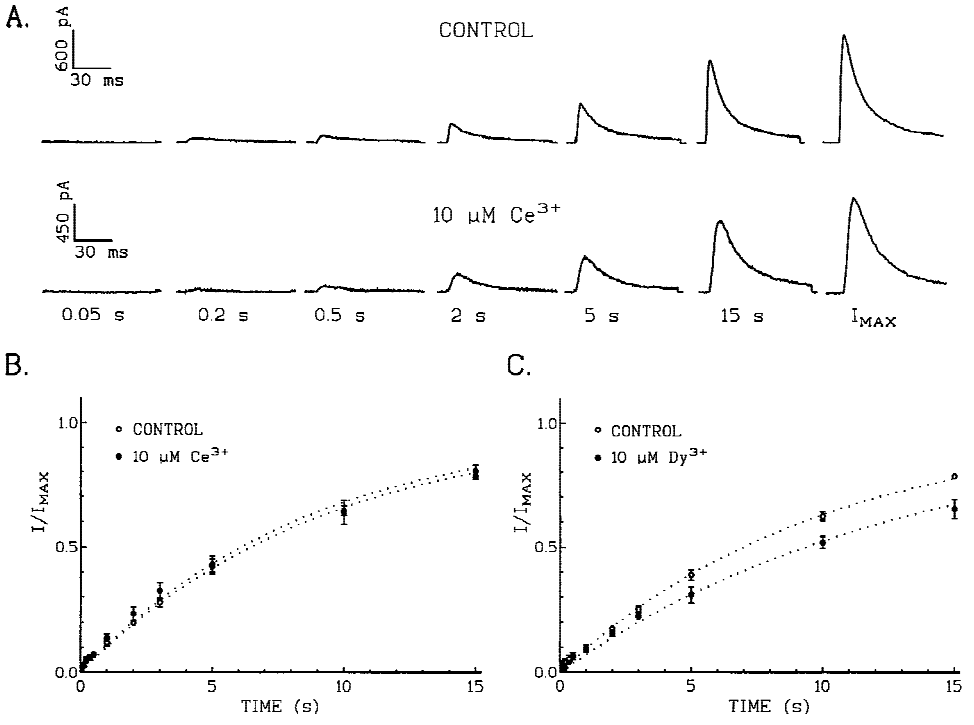

Fig. 7. Effect of Ln^{3+}s on recovery kinetics. Time-dependent recovery of I_A (inactivated by a 30-sec prepulse to −20 mV) was monitored by applying voltage steps to +20 mV after stepping to −80 mV for periods ranging from 0.05 to 30 sec. After measuring recovery in control saline, cells were superfused with Ce^{3+} or Dy^{3+} and recovery was against measured. (*A*) Current traces show I_A at indicated times after switching from the inactivating prepulse potential of −20 mV to the recovery potential of −80 mV before and after superfusing 10 μM Ce^{3+}. (*B*) Temporal pattern of I_A recovery. Peak current amplitudes normalized to maximum current (I/I_{max}) are plotted against time at recovery potentials of −80 mV before and after exposing cell to Ce^{3+} (*B*) or Dy^{3+} (*C*). Values are mean ± SEM, for 3 separate experiments. Data points were fit to a single exponential function of the form $I/I_{max} = 1 - \exp(-T/\tau_r)$.

ionic radius, particularly for the larger elements. The potency of Ln^{3+} as T-type Ca^{2+} channel antagonists was reduced by Ca^{2+}, indicative of competitive antagonism, between the blockers and permeant ion for a common binding site (Mlinar & Enyeart, 1993). To determine whether Ln^{3+} ions compete with Ca^{2+} for binding sites on I_A K^+ channels, the concentration-dependent inhibition of I_A by Ce^{3+} was compared in saline containing nominally 0, or 2 mM $CaCl_2$. The absence of $CaCl_2$ (replaced with equimolar $MgCl_2$) had no effect on the concentration-dependent reduction in I_A produced by Ce^{3+} (Fig. 11). In standard saline (2 mM $CaCl_2$), $CeCl_2$ suppressed I_A with an EC_{50} of 28.0 ± 4.1 μM ($n = 7$), compared to 32.1 ± 2.8 μM ($n = 7$) in ''zero Ca^{2+} saline''. The potency of $CeCl_3$ also was not increased when $CaCl_2$ and $MgCl_2$ were each reduced from 2.0 mM to 0.2 mM ($n = 3$) (*data not shown*).

The failure of Ca^{2+} removal to alter Ce^{3+} inhibition of I_A amplitude indicated a fundamental difference between the interaction of Ln^{3+}s with I_A K^+ and T-type Ca^{2+} channels. To further investigate this point, we examined the effect of the potent Ln^{3+} Ho^{3+}, Er^{3+}, and Gd^{3+} on T-type Ca^{2+} current recorded from rat C cells or bovine AZF cells. At a concentration of 100 nM, Ho^{3+} inhibited T-type Ca^{2+} current by approximately 50%, but produced no measurable slowing of I_T activation kinetics (Fig. 12*A* and *B*). Similarly, Er^{3+} (100 nM) and Gd^{3+} (100 nM) significantly inhibited T-type Ca^{2+} current in thyroid C cells (Fig. 12*C*) and AZF cells (Fig. 12*D*) without altering activation kinetics. In Fig. 12*C*, the $\tau_{1/2}$ for T current activation was 5.8 msec both in control saline and after superfusing 100 nM Er^{3+}. In Fig. 12*D*, $\tau_{1/2}$ in control saline and in the presence of 100 nM Gd^{3+} was 4.7 msec.

Discussion

In this study, we discovered that 10 Ln^{3+} elements suppress I_A K^+ current, slow activation kinetics, and alter the voltage-dependence of steady-state activation and inactivation with a potency that varies inversely with Ln^{3+} ionic radius. Voltage-dependent gating and kinetic parameters were not all affected. Channel closing, inactivation, and recovery kinetics were relatively insensitive to the Ln^{3+}s. The potency of the Ln^{3+} elements in inhibiting I_A current was independent of external Ca^{2+}. In contrast to their dramatic slowing of I_A activation

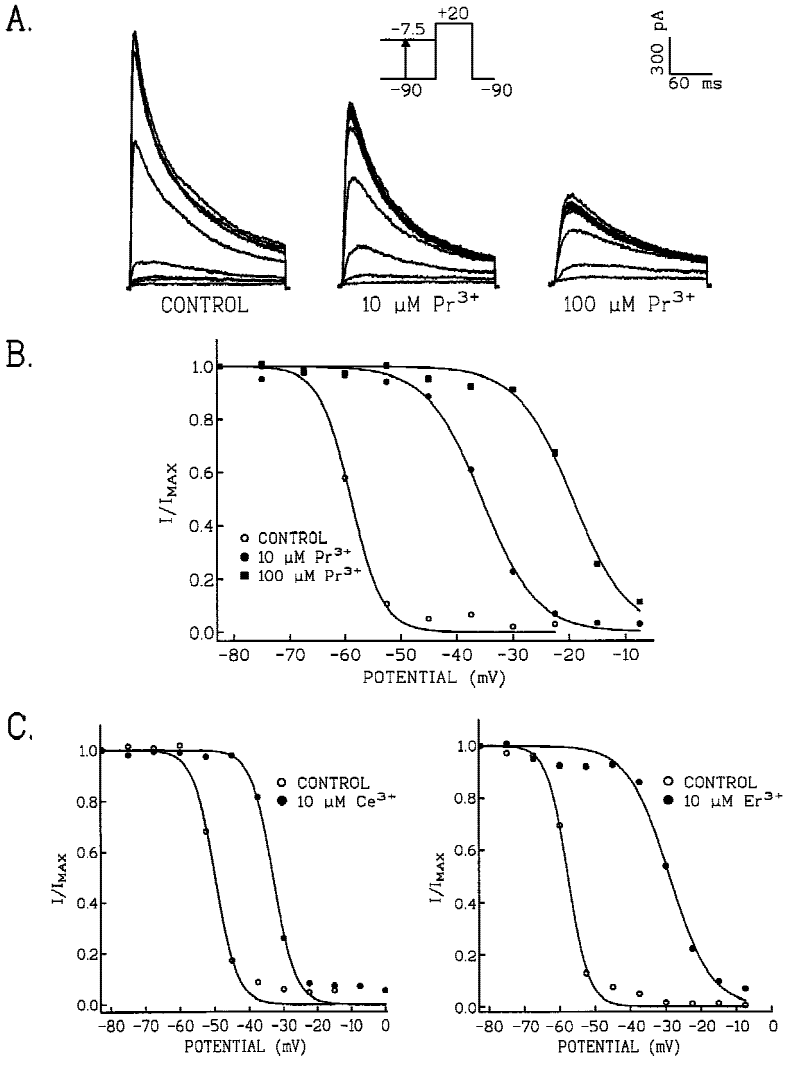

Fig. 8. Effect of Ln^{3+}s on voltage-dependent steady-state inactivation. I_A was activated by voltage steps to +20 mV after 10-sec conditioning pulses to potentials between −90 and −7.5 mV in 7.5 mV increments. Steady-state inactivation curves (or availability curves) were obtained by best fits of data to an expression of the form: $I = I_{max}/[1 + \exp(v - v_{1/2})/K]$, where I is measured current amplitude, I_{max} is the maximal I, v is the conditioning potential, $v_{1/2}$ is the potential at which half of the channels are available for activation and K is the slope factor. (*A* and *B*) Traces and corresponding steady-state inactivation curves recorded in control saline and after superfusing cell with 10 μM and then 100 μM Pr^{3+}. (*C*) Steady-state inactivation curves for individual cells obtained before and after 10 μM Ce^{3+} (left) or 10 μM Er^{3+} (right). Ce^{3+} shifted $v_{1/2}$ from −49.9 to −33.0 mV while Er^{3+} shifted $v_{1/2}$ from −54.8 to −28.9 mV.

kinetics, Ln^{3+}s inhibit T-type Ca^{2+} channels in AZF cells and thyroid C cells without slowing activation kinetics.

Mechanism of I_A Inhibition by Ln^{3+}s

Although Ln^{3+} inhibit both I_A K^+ current and T-type Ca^{2+} current with a potency that varies inversely with the ionic radius, fundamental differences in their respective mechanisms of channel modulation are apparent. Specifically, Ln^{3+}s slow I_A activation kinetics and shift the voltage dependence of activation and steady-state inactivation. In contrast, Ln^{3+}s failed to alter activation kinetics of T channels in AZF cells or thyroid C cells. Previously, we had demonstrated that La^{3+} blocks T-type Ca^{2+} channels in C cells without altering the voltage-dependence of steady-state inactivation (Mlinar & Enyeart, 1993). While inhibition of I_A by Ln^{3+}s was not enhanced by Ca^{2+} removal, Ca^{2+} reduced the potency of Ln^{3+}s as T-type Ca^{2+} antagonists, indicative of competitive antagonism between the blocker and permeant ion for a binding site.

These results suggest that Ln^{3+}s block T-type Ca^{2+} channels by occlusion of the pore upon binding to a Ca^{2+} site located outside of the membrane electric field. In contrast, Ln^{3+}s modulate I_A K^+ channels through interaction with a non-Ca^{2+} specific site located within the membrane electric field. While the Ln^{3+}s alter selected voltage-dependent gating and kinetic parameters, the extent to which these agents affect permeation through pore occlusion is not clear. In this regard, the marked slowing of activation kinetics and the rightward shift in the voltage dependence of I_A channel activation would both act to reduce I_A current amplitude to an extent dependent on the test potential.

In a simplified gating scheme, I_A channels travel from closed to open, and finally, to the inactivated state during the course of a depolarizing voltage step:

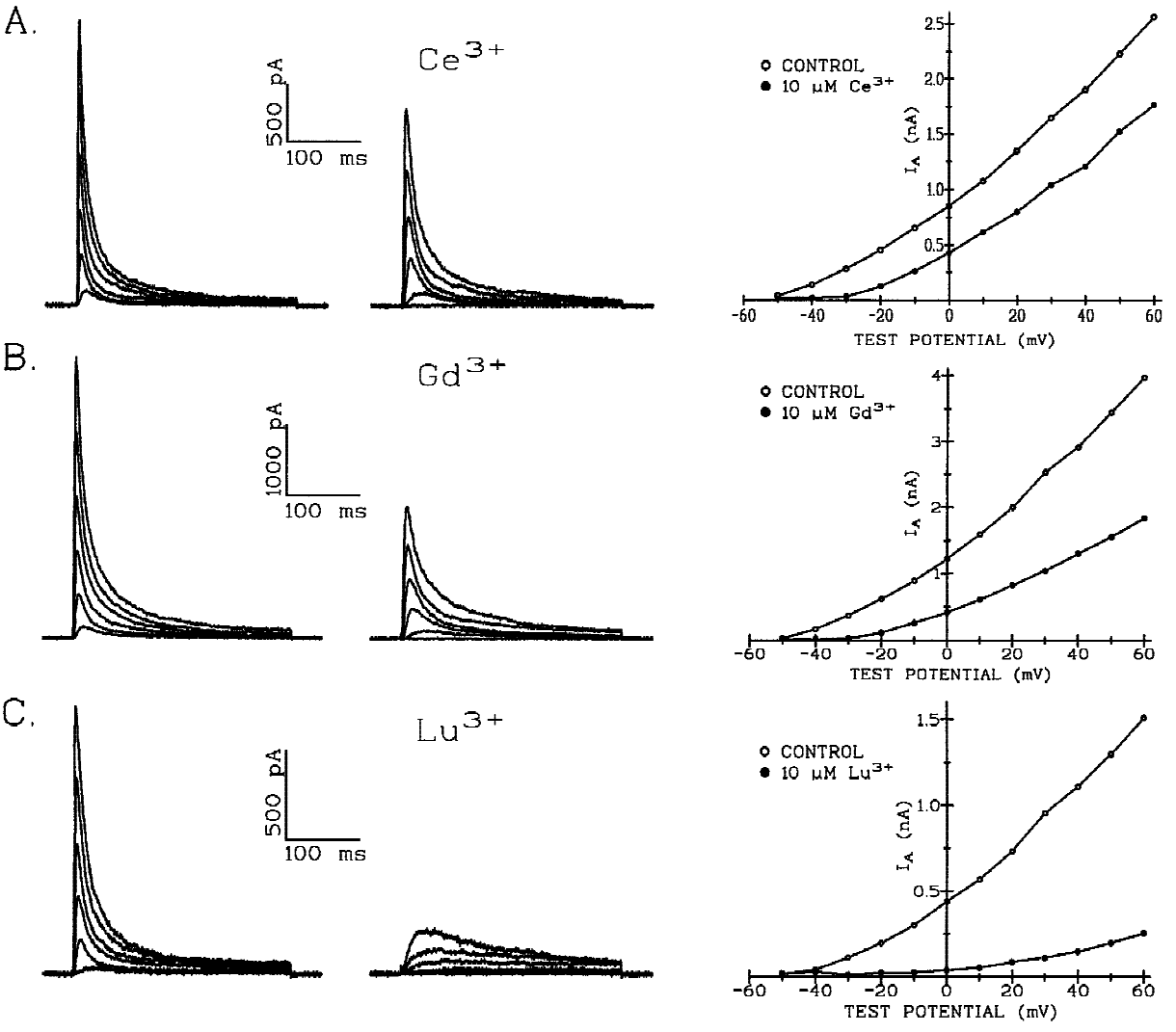

Fig. 9. Effects of Ln^{3+}s on I_A current voltage relationships. I_A K^+ currents were activated from −80 mV by voltage steps applied at 30-sec intervals to potentials between −50 and +60 mV before and after superfusing Ce^{3+} (10 μM) (A), Gd^{3+} (10 μM) (B), or Lu^{3+} (10 μM) (C). Peak I_A current amplitudes are plotted against test potentials.

$$C \xrightarrow{k_a} O \xrightarrow{k_i} I$$

By slowing activation kinetics (k_a) without altering inactivation kinetics (k_i), Ln^{3+}s reduce the maximum number of channels that are simultaneously open during a depolarizing voltage step. Consequently, peak current which is directly proportional to the number of open channels is reduced. The extent of peak current reduction would depend on the relative values of k_a and k_i. In the extreme case, with marked reduction of k_a, few channels would accumulate in the open state and I_A would be dramatically reduced. Further, Ln^{3+}-induced reduction of I_A would be blunted at more positive test potentials where activation is accelerated while k_i is unchanged.

By shifting the fraction open curve to the right on the voltage axis, the Ln^{3+}s would also inhibit I_A current by an amount that would vary with the magnitude of the shift as well as the test voltage. In general, the inhibition of I_A by Ln^{3+}s would decrease at progressively more positive voltages where the fraction open could still approach unity.

Therefore, the Ln^{3+}-induced reduction in I_A amplitude produced by slowed activation kinetics and shifts in voltage dependence of activation would both be proportionately less at more positive test voltages where activation is accelerated and the fraction of open channels increased. When *IV* relationships were recorded in the presence of Ln^{3+}s, we did observe that fractional inhibition of I_A decreased at progressively more depolarized test potentials.

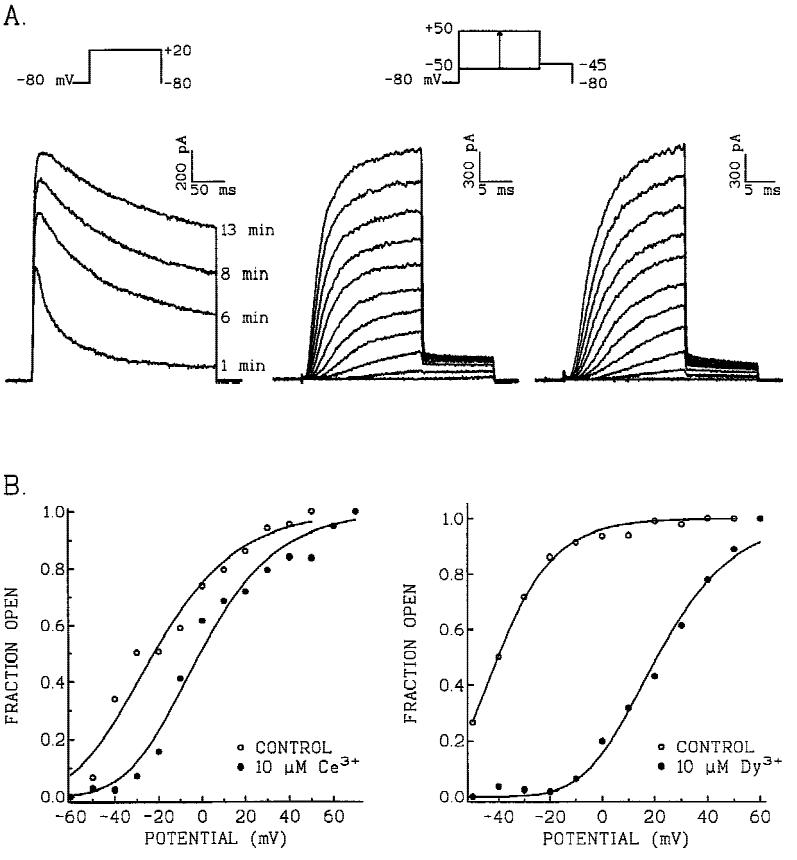

Fig. 10. Effect of Ln^{3+}s on voltage-dependent steady-state activation of I_A (*A* and *B*). I_A currents were recorded with a pipette containing standard pipette solution supplemented with 1 mM ATP-γ-S in place of ATP. This dramatically slowed I_A inactivation kinetics within 13 min (*A*), left traces. The effect of Ce^{3+} (10 μM) and Dy^{3+} (10 μM) on voltage-dependence of I_A activation was measured by recording tail currents at a constant potential (−50 mV) after applying activating test pulses to various potentials between −50 and +60 mV, before and after superfusing cells with either Ln^{3+}, (*A*) middle and right traces. (*B*) Tail current amplitudes were normalized and plotted as the fraction of open channels against test potential. Data points were fit with a Boltzmann expression of the form: Fraction Open $= 1/[1 + \exp(v_{1/2} - v)/K]^4$.

If Ln^{3+}s modulate I_A current only by slowing voltage-dependent activation kinetics and by inducing a rightward shift in the fraction open curve, then the total current integrals measured in response to a voltage step of sufficient size and duration should be equal, in the absence or presence of Ln^{3+}s. In the presence of 10 μM Ce^{3+}, the I_A current integral measured at +60 mV in experiments such as those shown in Fig. 9*A* was 104 ± 4% ($n = 3$) of the corresponding control value. For 10 μM Gd^{3+}, the I_A current integral measured only 80% of its control value. For smaller Ln^{3+}s, the I_A current integral was further suppressed.

Thus, although the actions of the larger Ln^{3+}s could all be attributed to the effects on gating described above it is possible that these agents might also alter ion permeation. In this regard, the smaller, more potent Ln^{3+}s markedly inhibited I_A current even at test potentials of at least +60 mV. It is difficult to determine whether this reduction in current stemmed from an action on ion permeation or an extreme rightward shift in the fraction open curve such that open probability did not approach unity even at +60 mV.

Inferences Regarding the Ln^{3+} Binding Site

Ca^{2+}-binding to specific sites on some K^+ channels may function critically in controlling the gating and permeation of these channels (Armstrong & Lopez-Barneo, 1987; Armstrong & Cota, 1990). It is unlikely that such a site exists on I_A channels since omission of Ca^{2+} from external saline did not affect I_A function. Therefore, it is unlikely that Ln^{3+}s interact with such a Ca^{2+}-specific site on I_A channels. The insensitivity of Ln^{3+} inhibition of I_A amplitude to complete removal of all external Ca^{2+} supports this conclusion. Ln^{3+}s bind to specific sites on some proteins where they cannot be displaced by Ca^{2+} (Dower et al., 1975; Stefanini et al., 1983). Other proteins have two separate Ln^{3+} binding sites, only one of which accepts Ca^{2+} (Rubsamen et al., 1976; Williams & Turtle, 1984). Our results indicate that Ln^{3+}s bind to a specific site on I_A channels that is not occupied by Ca^{2+} under physiological conditions.

Cationic radius is an important variable that determines the affinity and rate of ion interactions with protein binding sites (Tew, 1977; Tam & Williams, 1985). Assuming that the EC_{50}s that we measured provide a good approximation of the Ln^{3+}s affinity for I_A channels, these results demonstrate a progressive decrease in the affinity of larger Ln^{3+}s for the binding site. Ln^{3+}s with ionic radii closest to that of Ca^{2+} (1.12 Å) are least potent with respect to modulating I_A amplitude and gating. This data would again argue against Ln^{3+} binding to a Ca^{2+}-specific site on I_A channels. However, Ln^{3+}s inhibit T-

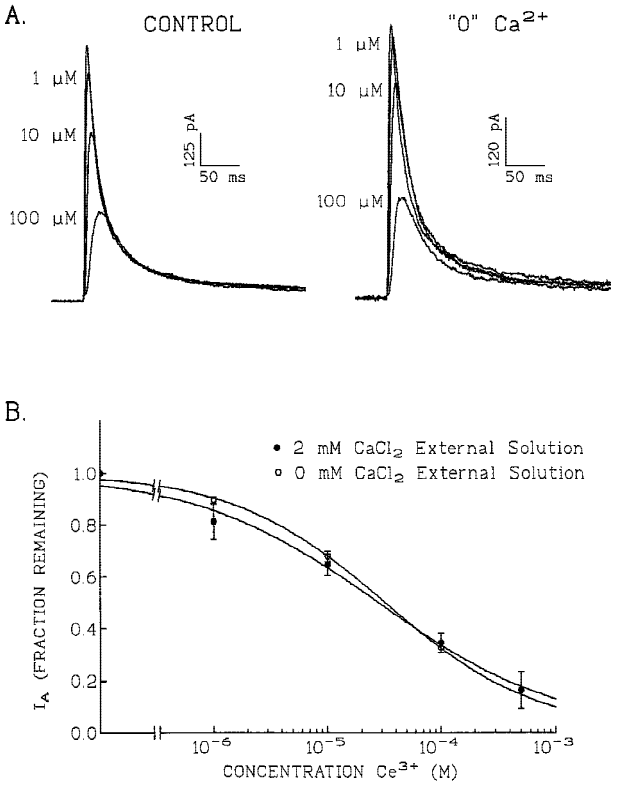

Fig. 11. Reduction of I_A by Ce^{3+} is independent of Ca^{2+}. I_A current was recorded at 30-sec intervals in response to voltage steps to +20 mV in control saline or in saline where $CaCl_2$ was replaced with $MgCl_2$ (''0'' Ca^{2+}). After recording control currents in either of these two solutions, $CeCl_3$ was superfused at concentrations of 1, 10, and 100 μM. (*A*) Traces show averaged currents at the indicated Ce^{3+} concentrations after steady-state inhibition was achieved. (*B*) Inhibition curves for Ce^{3+}. Data obtained in experiments as described above. Points are normalized mean values obtained in either 4 (2 mM $CaCl_2$) or 7 (0 mM $CaCl_2$) separate experiments. Inhibition curves are best fits of the data to an equation of the form: $Y = 1/[1 + (X/EC_{50})^h]$ where Y is the fraction of control current remaining after the addition of Ce^{3+}, and X is the Ce^{3+} concentration. EC_{50}s for Ce^{3+} estimated from the fits were 28.0 ± μM and 32.1 ± μM for control and ''0'' Ca^{2+} solutions, respectively.

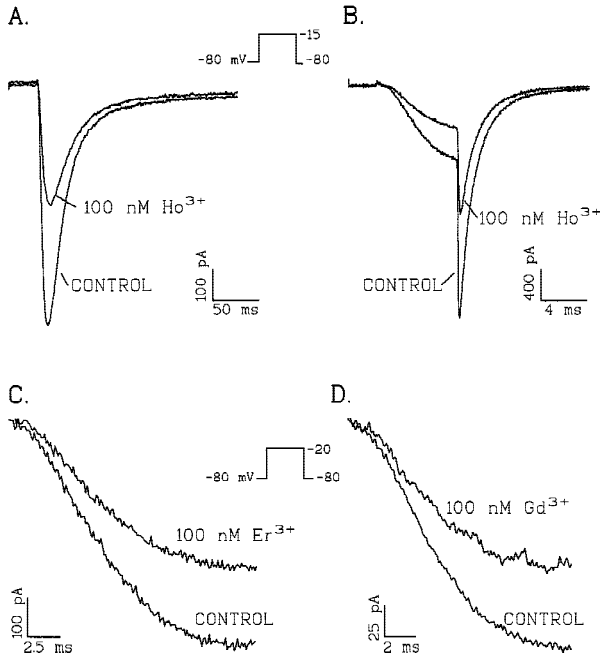

Fig. 12. Effect of Ln^{3+} of T-type Ca^{2+} current amplitude activation kinetics. T-type Ca^{2+} currents were activated by long (300 msec) (*A*) or short (30 msec) (*B,C,D*) voltage steps to −15 or −20 mV applied from a holding potential of −80 mV at 30-sec intervals. Records show currents after steady-state block was achieved with Ho^{3+} (*A* and *B*), Er^{3+} (*C*), or Gd^{3+} (*C*), each at 100 nM. Recordings in *A–C* are from thyroid *C* cells, those in *D* are from AZF cells. (*C*) and (*D*) show activating portion of T-type current. Cutoff frequency is 10 KHz.

type Ca^{2+} channels with this same order of potency through competitive interaction with an apparent Ca^{2+}-binding site (Mlinar & Enyeart, 1993). The Ln^{3+} binding site on T-type Ca^{2+} channels has a 100-fold higher affinity for Ln^{3+} than the binding site on A-type channels. Although the Ln^{3+} binding sites on T- and A-type channels are clearly distinct, it seems apparent that the measured affinity of Ln^{3+} of varying ionic radii for binding sites does not allow prediction of Ca^{2+} affinity.

The affinity sequences of Ln^{3+} for proteins and various biological preparations are frequently different from that which we observed on I_A current. Maximal affinity for larger elements or for those in the middle of the lanthanide series have often been observed (Nieboer, 1975; dos Remedios, 1981; Evans, 1990) reflecting the apparent diversity of Ln^{3+}-binding sites on proteins.

Ln^{3+}s and I_A Gating

With regard to mechanism, the Ln^{3+}s could alter voltage-dependent parameters by any of several mechanisms. According to Surface-Potential Theory, divalent and trivalent cations alter voltage-dependent gating parameters by screening of negative surface charges on the membrane, thereby changing the effective electric field across the membrane (*see* Hille, 1992 for a discussion). At least two lines of evidence argue strongly that Ln^{3+}-induced changes in modulation of I_A gating did not occur through surface charge screening. First, surface charge theory predicts that all voltage-dependent gating parameters should be shifted equally along the voltage axis. Ln^{3+}s dramatically shifted voltage-dependent activation and inactivation, as well as the kinetics of I_A activation but had little effect on deactivation and recovery kinetics. Further, the smaller Ln^{3+}s produced marked effects on I_A at concentrations as low as 1 μM. Since Mg^{2+} and Ca^{2+} were present at millimolar concentrations in these experiments, the total change in surface potential intro-

duced by the Ln^{3+}s would be insignificant and could not account for the large shifts in gating parameters.

Other researchers have also found that La^{3+} shifts voltage-dependent gating parameters for Na^+ and K^+ channels nonuniformly and even in an opposite direction (Armstrong & Cota, 1990; Watkins & Mathie, 1994). Earlier studies with divalent cations such as Zn^{2+} produced similar results and led Gilly and Armstrong to propose that these cations bind to specific negative charges of the gating apparatus, stabilizing the closed state of the channel (Gilly & Armstrong, 1982). While Zn^{2+} slows activation, it dissociates during this process and deactivation is not altered. In this regard, it has been reported that both divalent cations such as Zn^{2+} and the trivalent La^{3+} slow inactivation kinetics of A-type K^+ currents (Spires & Begenisich, 1994; Watkins & Mathie, 1994). Our results suggest that this effect may be generated indirectly through slowed activation kinetics.

Overall, the major effects of Ln^{3+} on I_A gating, including shifts in the voltage dependence of activation, inactivation and marked slowing of activation kinetics, can each be explained by a model similar to Gilly and Armstrong's. This assumes that Ln^{3+}s bind to sites on the gating apparatus, stabilizing the closed state of the channel. By lowering the energy of the closed state, Ln^{3+}s increase the size of the energy differences separating closed and open conformations of the channel (*see* Gilly and Armstrong (1982) for a complete discussion).

In addition to altering channel gating, Ln^{3+}s may affect I_A permeation by a separate mechanism. The reduction of I_A amplitude of Ln^{3+}s, particularly those with smaller radii, could not be overcome by strong depolarizations that largely negated shifts in voltage-dependent gating and kinetics produced by these elements. Thus, a direct effect of Ln^{3+} on ion permeation may occur.

In summary, Ln^{3+} elements interact with specific binding sites on I_A K^+ channels to modulate gating and kinetics with a potency that is a reciprocal function of their ionic radii. Compared to other organic K^+ antagonists, such as 4-amino pyridine which is frequently used to inhibit A-type currents, the smaller Ln^{3+}s are at least 100-fold more potent. Because of their potency, Ln^{3+} elements can be used to study gating and permeation at low concentrations, where surface charge screening effects are negligible. Finally, it is notable that Ln^{3+}s modulate transient K^+ and Ca^{2+} currents in AZF cells with the identical order of potential, but by different mechanisms. Ln^{3+} are often used to demonstrate the specific involvement of Ca^{2+} channels in cellular functions such as secretion. The ability of these elements to dramatically alter the function of voltage-gated K^+ channels at micromolar concentrations indicates that other possible sites of action should be considered.

This work was supported by National Institute of Diabetes and Digestive and Kidney grant DK-47875 and by National American Heart Association Grant-in-aid 94011740 to JJE.

References

Armstrong, C.M., Cota, G. 1990. Modification of sodium channel gating by lanthanum. *J. Gen. Physiol.* **96:**1129–1140

Armstrong, C.M., Lopez-Barneo, J. 1987. External calcium ions are required for potassium channel gating in squid neurons. *Science* **236:**712–714

Begenisich, T. 1988. The role of divalent cations in potassium channels. *TINS* **11:**270–273

Biagi, B.A., Enyeart, J.J. 1991. Multiple calcium currents in a thyroid C-cell line: biophysical properties and pharmacology. *Am. J. Physiol.* **260:**C1253–C1263

Biedermann, G., Ciavatta, L. 1961. Studies on the hydrolysis of metal ions: part 35, the hydrolysis of lanthanum, La^{3+}. *Acta Chemica Scandinavica* **15:**1347–1366

Brooks, S.P.J., Storey, K.B. 1992. Bound and determined: a computer program for making buffers of defined ion concentrations. *Anal. Biochem.* **201:**119–126

dos Remedios, C.G. 1981. Lanthanide ion probes of calcium-binding sites on cellular membranes. *Cell Calcium* **2:**29–51

Dower, S.K., Dwek, R.A., McLaughlin, A.C., Mole, L.E., Press, E.M., Sunderland, C.A. 1975. The binding of lanthanides to non-immune rabbit immunoglobulin G and its components. *Biochem. J.* **149:**73–82

Enyeart, J.J., Mlinar, B., Enyeart, J.A. 1996. Adrenocorticotropic hormone and cAMP inhibit noninactivating K^+ current in adrenocortical cells by an A-kinase-independent mechanism requiring ATP hydrolysis. *J. Gen. Physiol.* **108:**251–264

Evans, C.H. 1990. Chemical Properties of Biochemical Relevance. *In:* Biochemistry of the Lanthanides, pp. 9–46. Plenum Press, New York

Gilly, W.F., Armstrong, C.M. 1982. Divalent cations and the activation kinetics of potassium channels in squid giant axons. *J. Gen. Physiol.* **79:**965–996

Gospodarowicz, D., III, C.R., Hornsby, P.J., Gill, G.N. 1977. Control of bovine adrenal cortical cell proliferation by fibroblast growth factor. Lack of effect of epidermal growth factor. *Endocrinology* **100:**4:1080–1089

Hamill, O.P., Marty, A., Neher, E., Sakmann, B., Sigworth, F.J. 1981. Improved patch clamp techniques for high resolution current recording from cells and cell-free membrane patches. *Pfluegers Arch.* **391:**85–100

Hille, B. 1992. Modifiers of Gating. *In:* Ionic Channels of Excitable Membranes. pp. 445–471. Sinauer Associates, Sunderland, MA

Lansman, J.B. 1990. Blockade of current through single calcium channels by trivalent lanthanide cations. *J. Gen. Physiol.* **95:**679–696

Mayer, M.L., Sugiyama, K. 1988. A modulatory action of divalent cations on transient outward current in cultured rat sensory neurones. *J. Physiol.* **396:**417–433

Mlinar, B., Biagi, B.A., Enyeart, J.J. 1993. Voltage-gated transient currents in bovine adrenal fasciculata cells I: T-type Ca^{2+} current. *J. Gen. Physiol.* **102:**217–237

Mlinar, B., Enyeart, J.J. 1993*a*. Voltage-gated transient currents in bovine adrenal fasciculata cells II: A-type K^+ current. *J. Gen. Physiol.* **102:**239–255

Mlinar, B., Enyeart, J.J. 1993*b*. Block of current through T-type calcium channels by trivalent metal cations and nickel in neural rat and human cells. *J. Physiol.* **469:**639–652

Nieboer, E. 1975. The lanthanide ions as probes in biological systems. *Structure and Bonding* **22:**1–47

Rubsamen, H., Hess, G.P., Eldefrawi, A.T., Eldefrawi, M.E. 1976. Interaction between calcium and ligand-binding sites of the purified acetylcholine receptor studied by use of fluorescent lanthanide. *Biochem. Biophys. Res. Commun.* **68:**56–62

Shannon, R.D. 1976. Revised effective ionic radii and systematic studies of interatomic distances in halides and chalcogenides. *Acta Crystallographica* **A32:**751–767

Spires, S., Begenisich, T. 1994. Modulation of potassium channel gating by external divalent cations. *J. Gen. Physiol.* **104:**675–692

Stefanini, S., Chiancone, E., Antonini, E., Finazzi-Agro, A. 1983. Binding of terbium to apoferrin: a fluorescence study. *Arch. Biochem. Biophys.* **222:**430–434

Tam, S.-C., Williams, R.J.P. 1985. Electrostatics and biological systems. *Structure and Bonding* **63:**103–151

Tew, W.P. 1977. Use of the coulombic interactions of the lanthanide series to identify two classes of Ca^{2+} binding sites in mitochondria. *Biochem. Biophys. Res. Commun.* **78:**624–630

Watkins, C.S., Mathie, A. 1994. Modulation of the gating of the transient outward potassium current of rat isolated cerebellar granule neurons by lanthanum. *Pfluegers Arch.* **428:**209–216

Williams, P.F., Turtle, J.R. 1984. Terbium, a fluorescent probe for insulin receptor binding. Evidence for a conformational change in the receptor protein due to insulin binding. *Diabetes* **33:**1106–1111

Williams, R.J.P. 1982. The chemistry of lanthanide ions in solution and in biological systems. *Structure and Bonding* **50:**79–119